

Review

Nitrogen Fixation via Plasma-Assisted Processes: Mechanisms, Applications, and Comparative Analysis—A Comprehensive Review

Angelique Klimek ^{1,2} and Davin G. Piercey ^{2,3,4,*}

¹ School of Chemical Engineering, Purdue University, 480 Stadium Mall Drive, West Lafayette, IN 47906, USA; klimek0@purdue.edu

² Purdue Energetics Research Center, Purdue University, 205 Gates Road, West Lafayette, IN 47906, USA

³ School of Materials Engineering, Purdue University, 205 Gates Road, West Lafayette, IN 47906, USA

⁴ School of Mechanical Engineering, Purdue University, 585 Purdue Mall, West Lafayette, IN 47906, USA

* Correspondence: dpiercey@purdue.edu

Abstract: Nitrogen fixation, the conversion of atmospheric nitrogen into biologically useful compounds, is crucial for sustaining biological processes and industrial productivity. Recent advances have explored plasma-assisted processes as an innovative approach to facilitate nitrogen fixation. This review offers a comprehensive summary of the development, current state of the art, and potential future applications of plasma-based nitrogen fixation. The analysis encompasses fundamental principles, mechanisms, advantages, challenges, and prospects associated with plasma-induced nitrogen fixation.

Keywords: nitrogen fixation; nitric oxide; plasma reactors; plasma catalysis; energy efficiency



Citation: Klimek, A.; Piercey, D.G. Nitrogen Fixation via Plasma-Assisted Processes: Mechanisms, Applications, and Comparative Analysis—A Comprehensive Review. *Processes* **2024**, *12*, 786. <https://doi.org/10.3390/pr12040786>

Academic Editor: Francesco Parrino

Received: 22 February 2024

Revised: 5 April 2024

Accepted: 8 April 2024

Published: 13 April 2024



Copyright: © 2024 by the authors. Licensee MDPI, Basel, Switzerland. This article is an open access article distributed under the terms and conditions of the Creative Commons Attribution (CC BY) license (<https://creativecommons.org/licenses/by/4.0/>).

1. Introduction

Nitrogen is a crucial element of numerous biomolecules, such as ATP, DNA, RNA, and amino acids. Nitrogen is essential for synthesizing proteins, photosynthesis, genetic character determination, and all other vital processes in life [1–3]. It can be found in a variety of forms, both organic and inorganic, that can be encountered in nature. It is also required to synthesize numerous chemicals, including fertilizers, pharmaceuticals, explosives, and pigments [4]. Nitrogen N₂, which comprises 78% of atmospheric air, contains more than 99% of nitrogen globally [5]. However, since N₂ is chemically inert, most organisms cannot access it. Thus, it must first undergo a process referred to as nitrogen fixation to transform it into a reactive form (such as ammonia or nitrates). This procedure involves bonding elements such as O, H, and C to an N atom that originated from breaking the triple bond of N₂.

The most common form of nitrogen fixation worldwide is biological nitrogen fixation (BNF). However, because of its comparatively slow speed, the process cannot supply enough fertilizer to support the expanding population. According to a study conducted by the United Nations Food and Agriculture Organization (FAO), 9 million people remain hungry as there is a gap between global grain output and demand of 2.216 billion tons vs. 2.254 billion tons of grain [6]. The Haber-Bosch (H-B) process is the most commonly used commercial nitrogen fixation method. It generates ammonia through a chemical reaction involving hydrogen and nitrogen at high temperatures and pressures, utilizing heterogeneous catalysts. Up until 2010, more than 120 million tons of nitrogen per year were fixed using this process, with approximately 80% employed as fertilizer and the remaining 20% serving as feedstock for the synthesis of other nitrogen-containing compounds [7–9]. Industrial nitrogen fixation has played a pivotal role in exponentially increasing global food production to meet the demands of the world's fast-growing population. Studies

by Smil et al. and Erisman et al. reported that, by the end of the 20th century, about 40% of the world's population was utilizing fertilizers [7,10,11]. By 2008, this percentage had risen to 48% of the world's population, underscoring the substantial impact of industrial nitrogen fixation. Given the anticipated world population growth, there is an imminent and growing demand for fertilizers, emphasizing the critical need for continued development of industrial nitrogen fixation techniques [12].

Numerous attempts have been undertaken throughout history to artificially fix nitrogen, including the H-B process, the Frank-Carolo method [13–15], and the Birkland-Eyde (B-E) process [13,16–18]. Among these, the H-B process, developed by Fritz Haber and commercially implemented by Carl Bosch, is largely regarded as one of the largest and most notable developments of the 20th century. [10]. Ammonia is produced through the reaction of N_2 and H_2 at high temperatures (450–600 °C) and pressures (150–350 bar) in the presence of catalysts, as depicted in Figure 1. The H-B process has undergone extensive optimization over the past century, leveraging advancements in catalyst technology, the usage of natural gas as a feedstock instead of coal, and improved heat integration, among other factors. Consequently, this optimization has led to a reduction in energy usage to 0.48 MJ/mol of generated ammonia [19,20].

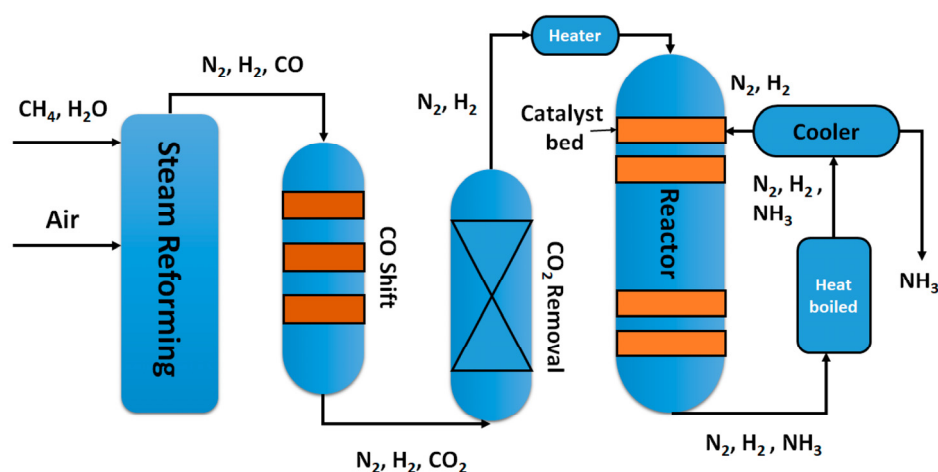


Figure 1. A flow scheme for the Haber-Bosch process. Reprinted with permission from Ref. [21].

Despite being the primary method for industrial nitrogen fixation, the H-B process is extremely energy-intensive and has adverse environmental impacts. This process requires 1–2% of the world's total energy and 2% of the total natural gas, resulting in 300 million metric tons of CO_2 emissions [19,22,23]. The H-B process is currently very close to its theoretical energy efficiency limits, with hydrogen generation via the thermal or catalytic cracking of fossil fuels at high temperatures and pressures over catalysts being the most energy-intensive aspect of the process. Consequently, improvements in catalyst technology are unlikely to significantly enhance energy efficiency [24]. As an alternative to natural gas as a hydrogen source, electricity-powered water splitting has been proposed. However, this technique is only viable if renewable electricity is employed, as it would otherwise result in an overall energy consumption of around 1.5 MJ/mol, which is 3-fold greater than the H-B process [20]. This is attributed to higher energy demands for H_2 production (360–480 kJ/mol [25]) compared to the steam methane reforming system. Improving the energy efficiency of nitrogen fixation would be highly advantageous both economically and environmentally, especially considering the rapidly expanding population and the depletion of natural resources. Consequently, ongoing research into sustainable nitrogen fixation techniques is evident in the literature, encompassing the advancement of plasma-assisted nitrogen fixation processes and the utilization of metallocomplex homogeneous catalysts.

Near the turn of the 20th century, as the world's supply of fixed nitrogen was almost depleted, Sir William Crookes, the President of the British Association at the time, called

attention to this issue. Sodium and potassium nitrate were the most extensively utilized agricultural fertilizers in Europe, in the form of bird droppings accumulated and solidified over millennia [26]. Plasma-assisted nitrogen fixation was among the first attempts at industrial nitrogen fixation. A significant quantity of electrical energy can cause gas to ionize, generating plasma [27–29]. A wide variety of pressures, temperatures, electron densities, and electron temperatures can result in the formation of plasma, making a universal approach to plasma classification challenging. Plasmas are divided into two types: high-temperature plasmas and low-temperature plasmas. The temperature of ions and electrons in high-temperature plasmas is roughly 10^7 K. Thermal and non-thermal low-temperature plasmas are established [30]. Electrons, ions, and background gas are all present in thermal plasma at a temperature of about 10^4 K. Thermal plasma is used in arc plasma and plasma torches. However, in non-thermal plasmas, due to their smaller mass, electrons are often at very high temperatures of the order of 10^5 K. In contrast, ions and background gas are at room temperature. The first industrial method utilized for nitrogen fixation was the Birkland-Eyde process, which in 1903 produced thermal plasma at a high temperature for the generation of NO using an electrical arc discharge [31,32]. The airflow passed via an arc discharge zone before being quenched with water and going through a succession of adsorption stages, yielding roughly 1% nitric oxide with an energy consumption of 3.4–4.1 MJ/mol HNO_3 , as shown in Figure 2 [31,32].

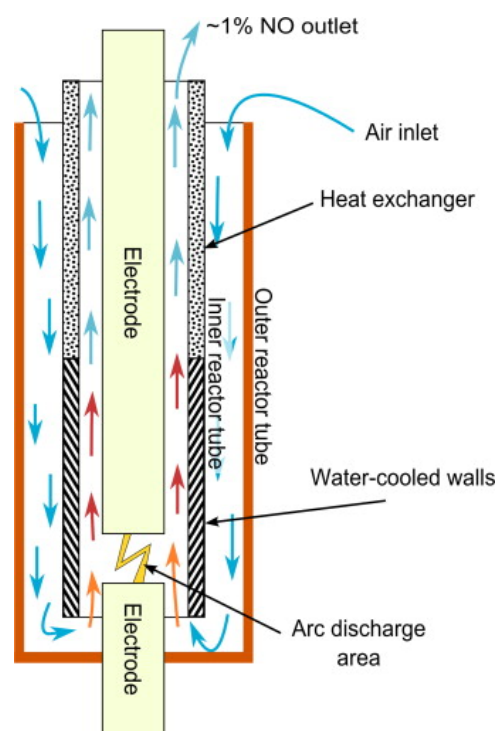


Figure 2. Scheme of Birkland–Eyde arc discharge apparatus. Reprinted with permission from Ref. [20].

Thermodynamic reasoning can be used to rationalize thermal plasma NF by considering two opposing processes: (a) the creation of NO and (b) the atomization of molecules of nitrogen and oxygen [29,33]. N_2 and O_2 molecules predominate at lower temperatures; however, they dissociate into atoms at higher temperatures. The NO concentration reaches its maximum at around 3500 K, at 6.5% [33]. This low concentration suggests that, as opposed to N_2 oxidation, most of the energy is used for gas heating.

Regarding environmental concerns, plasma processes hold a significant advantage over the H-B process as they utilize abundant materials like air and water instead of expensive H_2 . Moreover, there is the potential for plasma processes to be fueled by electricity

produced using renewable resources, such as solar or wind. According to research by the International Energy Agency, silicon photovoltaics currently provide some of the cheapest electricity historically as a result of economies of scale, technological advancements in the production supply chain, increased productivity, and lower basic material costs [34]. Additionally, the procedure is sustainable, generating no waste or greenhouse gas emissions. However, as documented in the literature to date, the energy efficiency of thermal plasma is not competitive with the H-B process. Under speculative conditions of 20–30 bars, 3000–3500 K, and a cooling rate of 10^7 – 10^8 K/s, thermal plasma has a theoretical energy consumption of 0.86 MJ/mol of NO [35]. Non-thermal plasma utilization, however, has a theoretical limit of 0.2 MJ/mol (for NO_x synthesis) [35,36], a value lower than the limits of the H-B process; however, to date, this limit has not been reached, meaning there is still room for work in this field to reach the practical application. Furthermore, the non-thermal plasma technique offers numerous technical benefits, including quick reaction times, rapid control, and suitability for decentralized and small-scale production using intermittent energy sources like solar, which traditional H-B cannot use [29]. The advancement of plasma technology in recent decades has significantly influenced nitrogen fixation research, resulting in numerous discoveries being reported. While there have been other recent reviews in this field [37–41], the field of plasma-based nitrogen fixation is quickly growing, as seen in Figure 3, wherein 2023, almost seven times as many papers were published on this topic as in 2018. (Search results via Google Scholar using the search term “plasma based” and “nitrogen fixation”). This review focuses on important work in the field before the most recent years, as well as significant papers since then.

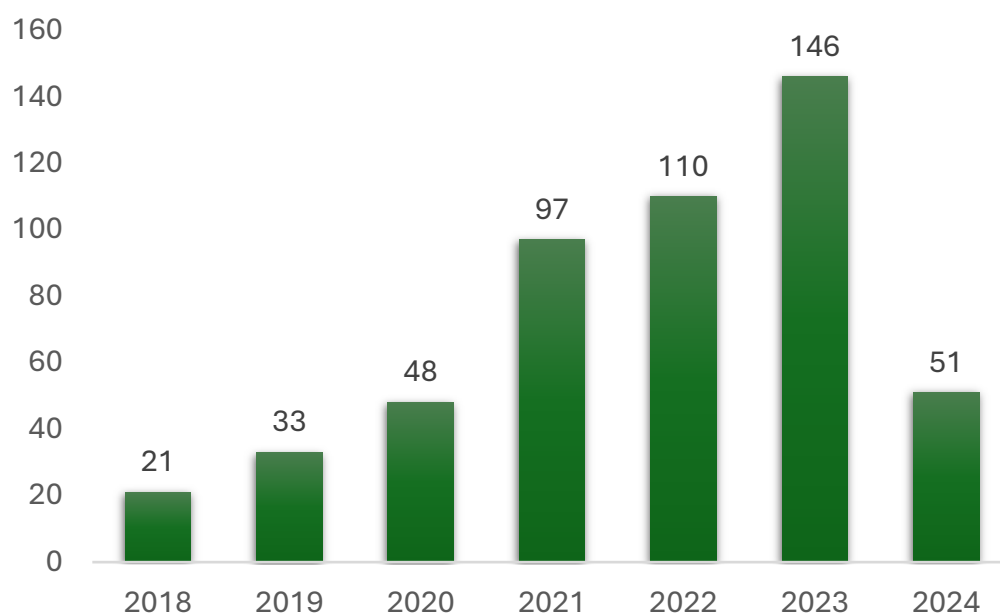


Figure 3. Number of results obtained via Google Scholar for publications on plasma-based nitrogen fixation by year published. The results had to include phrases “plasma-based” and “nitrogen fixation”.

2. Plasma N₂ Fixation

The general process for plasma nitrogen fixation involves the reaction of nitrogen with either hydrogen or oxygen, which results in the production of ammonia or nitrogen oxide (nitric acid). In the case of ammonia synthesis, kinetic reaction rates and nitrogen dissociation are greater at higher temperatures, whereas higher yields are obtained at lower temperatures. In addition to easily available nitrogen, costly hydrogen is required for plasma ammonia production. Air is an abundant and affordable raw material in the creation of plasma nitric oxide. Because of the high dissociation energy of nitrogen, high-temperature processing promotes NO reactions [42]. This review will focus on nitrogen fixation to form nitrogen oxides.

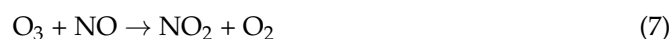
The reaction mechanism of NO_x formation follows the Zeldovich mechanism, which begins with the dissociation of N₂ in Equation (1) and O₂ in Equation (2):



This is followed by the stage of NO generation, as shown in Equations (3) and (4) below:



NO₂ can be created by oxygen radicals or ozone during continuous oxidation, as illustrated in Equations (5)–(7):



Various research groups have published a large number of studies on plasma nitrogen fixing due to the rapidly advancing developments in our understanding of plasma reaction kinetics [43–51]. Researchers have investigated the conversion of atmospheric nitrogen fixation into NO for laboratory-scale procedures utilizing air plasma [46,49,52,53], from N₂–O₂ mixtures [43,44,51,54], and in argon; argon–nitrogen and nitrogen plasma [47,54,55]. Following earlier studies on thermal plasma (i.e., the electric arc), other plasma types and plasma reactors have been examined for NO_x production [31,32,56,57]. This includes (pulsed) spark discharges [58–63], glow discharges [59,64], corona discharges [58,65], laser-produced discharges [66], radio-frequency crossed discharges [67], (packed bed) dielectric barrier discharges (DBD) [59,68–70], (pulsed) (rotating) (gliding) arc discharges [59,71–78], microwave (MW) discharges [54,79,80], and plasma jets in contact with water [81–91]. The reported energy consumption for a variety of plasma reactors is listed in Table 1. Energy consumption and plasma efficiency are difficult to compare between different authors and publications due to the existence of diverse quantification methods. Energy consumption is dependent on power and NO_x concentration. NO_x concentrations can be determined via Fourier-transform infrared spectroscopy (FTIR) [59,61,68,70,73,74], mass spectroscopy [71], chemiluminescence [66], ion chromatography chromatogram [65], as well as a nondispersive infra-red sensor with an ultra-violet sensor through a gas analyzer [56]. Power can be calculated by the Lissajous method [59,68], the numerical product of air density, room temperature, heat capacity of the air, and volume [66], numerically integrating the product of the voltage and current and multiplying by the frequency [61,65,70] where the current can be measured by the resistor method [56,71,73,74] or by a current coil [59]. Total power also varies between literature papers as the addition of power consumption to prepare pure oxygen gas from air to plasma power has been reported [74], or the placement of the measured variables varies from before the plasma vs. right before the power supply. All of these various methods used by various groups in the field can lead to uncertainty between results reported by various methods.

Table 1. Comparison of the energy used in plasma reactors to produce NO_x.

Plasma Type	Energy Consumption (MJ/mol N)	Reference
Electric arc (Birkeland–Eyde)	2.4–3.1	[31,33,57]
Spark discharge	20.27, 40, 1.9–4.4	[58,61,62]
Plate-to-plate ns-pulsed spark discharge	22.18–25.72	[63]
Pin-to-plane ns-pulsed spark discharge	5.0–7.7	[59]
Transient spark discharge	8.6	[60]
(Positive/negative) DC corona discharge	1057/1673	[58]
Pulsed corona discharge	186	[65]
Radio-frequency crossed discharge	24–108	[67]
Laser-produced discharge	8.9	[66]
Pin-to-plane DC glow discharge	7, 2.8–4.8	[59,92]
Pin-to-pin DC glow discharge	2.8	[64]
Dielectric barrier discharge	56–140, 20.7	[59,69]
Packed dielectric barrier discharge	18, 17–33	[68,70]
DC plasma arc jet	3.6	[72]
Propeller arc	4.2	[59]
Pulsed milli-scale gliding arc	2.8–4.8	[73,74]
Gliding arc plasmatron	3.6	[71]
Rotating gliding arc	2.5, 1.8, 0.67, 4.2, 2.1	[68,75–78]
Microwave plasma	3.76	[79]
Microwave plasma with catalyst	0.84	[54]
Electron cyclotron resonance	0.28	[80]

Various gliding arc (GA) reactor layouts have demonstrated potential for gas conversion applications [71,73–77,93–95]. GA plasmas have reduced electric fields of less than 100 Townsends (Td), resulting in electron energies of roughly 1 eV. Such electron energies are particularly advantageous for the vibrational excitation of gas molecules [93]. Wang et al. [74] researched NO_x formation mechanisms in a milli-scale (reactor width of 135 mm and a minimum discharge gap of 1.3 mm) GA reactor with pulsed power. Vervloessem et al. [71] examined the creation of NO_x in a flow gliding arc plasmatron (GAP) using a reverse vortex. Schematics of these gliding arc systems can be found in Figure 4. The results of the chemical kinetics modeling showed that vibrationally excited N₂ molecules can reduce the nonthermal Zeldovich process's energy barrier, allowing for more energy-efficient NO generation. Moreover, the lower N₂ vibrational levels, whose vibrational distribution function has a Boltzmann shape, undergo considerable thermal dissociation due to the high gas temperature (>3000 K). The fraction of gas treated by the GA plasma limits the total amount of N₂ conversion, even though the thermal reactions in GA reactors are highly efficient at high temperatures. Only 15% of the gas passes through the plasma arc in the GAP, and the remaining gas passes through the reactor without coming into contact with the plasma. [95,96]. Vervloessem et al. [71] reported a 1.5% NO_x yield at 3.6 MJ/mol N energy consumption. The authors demonstrated that by optimizing the reactor and avoiding the transmission of vibrational energy from N₂ to O₂, energy consumption could be reduced to 0.5 MJ/mol N; however, this finding must be investigated in practice [71]. Tsonev et al. [75] demonstrated that when pressure increases, the amount of NO_x produced increases dramatically, with a record-low EC of 1.8 MJ/mol N, a high production rate of 69 g/h, and a high selectivity (94%) of NO₂. The authors credit this enhancement to the enhanced thermal Zeldovich mechanism and a higher rate of NO oxidation relative to the back reaction of NO with atomic oxygen caused by the elevated pressure [75]. Chen et al. [77] found that the rotating gliding arc plasma can efficiently generate NO_x from a mixture of N₂ and O₂ or air, with low energy consumption and high processing capacity. The lowest energy consumption for NO_x production (4.2 MJ/mol N) is reached with a voltage of 10 kV, a gas flow rate of 12 L/min, and an O₂ concentration of 20%. The order of importance for process parameters concerning NO_x concentration is gas flow rate followed by O₂ concentration and applied voltage, while for energy consumption of NO_x

formation, the order is O_2 concentration followed by gas flow rate and applied voltage [77]. Muzammil et al. [76] showed that in a rotating gliding arc plasma, low specific energy input (SEI) leads to optimal energy efficiency and high NO selectivity. However, the largest production rate occurs at a high SEI. Their process has high NO selectivity (up to 95%) and low energy consumption (~ 48 GJ per tN) at 0.1 kJ L^{-1} SEI, which is equal to 0.67 MJ/mol N . Alphen et al. [78] focused on improving performance in a rotating gliding arc plasma by developing an “effusion nozzle”. The nozzle acted as a heat sink, limiting the breakdown of NO back into N_2 and O_2 due to the fast drop in gas temperature. This system allowed the achievement of higher NO_x concentrations of up to 5.9% while keeping the energy consumption low at 2.1 MJ/mol N .

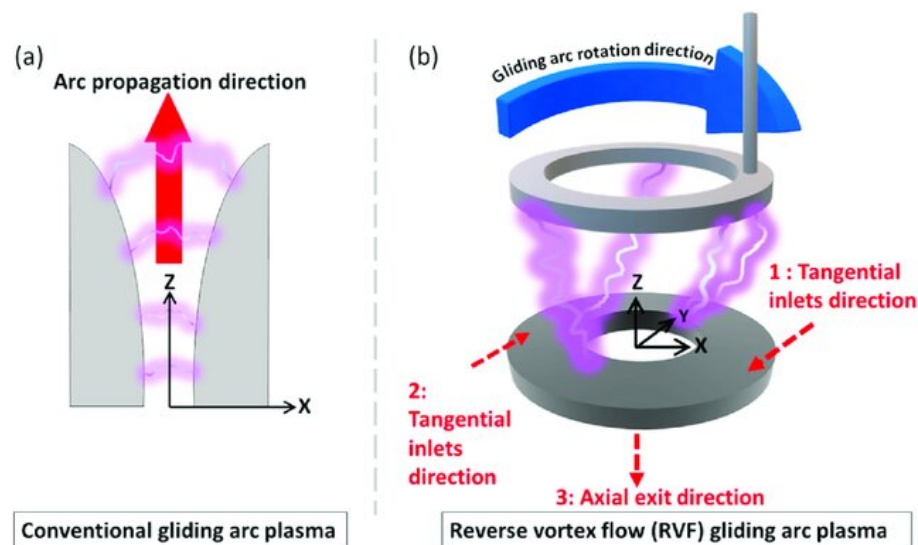


Figure 4. Schematic of gliding arc systems. (a) Conventional 2D gliding arc plasma. (b) Reverse vortex flow gliding arc plasma. Reprinted with permission from Ref. [97].

Janda et al. [60] investigated the generation of NO_x in a transient spark discharge. This type of spark discharge starts as a non-thermal plasma known as the streamer phase and transitions into quick spark current pulses that result in the production of a thermal plasma [98,99]. Because of the high electron density (approximately 10^{17} cm^{-3}), the spark phase is marked by significant chemical activity. Excited nitrogen molecules were detected via time-integrated emission spectroscopy in both the streamer and spark phases, and the energy consumed for NO_x generation was 8.6 MJ/mol N [60]. Pavlovich et al. [61] built a reactor that produced a spark-glow discharge, wherein the plasma discharge had both a glow (non-thermal plasma) and a spark (thermal plasma) phase in a single cycle. Schematics for a spark and glow discharge are illustrated in Figure 5. Pavlovich et al. changed the percentage of the glow phase by adjusting the voltage waveforms. With its high electron density and energy, the spark phase generated more NO, while the glow phase made it easier for NO_2 to develop. The production of NO_x required up to 40 MJ/mol N of energy. These plasma types often have a limited volume, which means that only a portion of the N_2 gas is exposed to the plasma, and consequently, only a small amount of NO_x is produced. Abdelaziz et al. [62] demonstrated that using a bipolar voltage at high frequencies in a spark discharge reactor increased NO_x production and efficiency by utilizing residual species. Enlarging the plasma zone (reaction channel) by increasing the electrode gap improves energy efficiency for the desired reaction. The limits of increasing the gap were overcome by introducing a floating electrode, resulting in increased NO_x generation (1.8–3.0%) and lower energy consumption ($1.9\text{--}4.4 \text{ MJ/mol N}$). Zhang et al. [63] used a plate-to-plate setup to create a nanosecond pulsed spark discharge for long-term nitrogen fixation under ambient circumstances. The airflow speeds ranged from 40 to 340 mL min^{-1} , resulting in an energy efficiency of $4\text{--}11 \text{ g kWh}^{-1}$ (equal to 22.18

MJ/mol N) and NO_x production concentrations of 960–10,900 ppm. Using optical emission spectroscopy and a chemical kinetics model, they discovered that the major intermediate species in NO_x reaction pathways are significantly influenced by plasma characteristics and species residence duration in spark discharges [63].

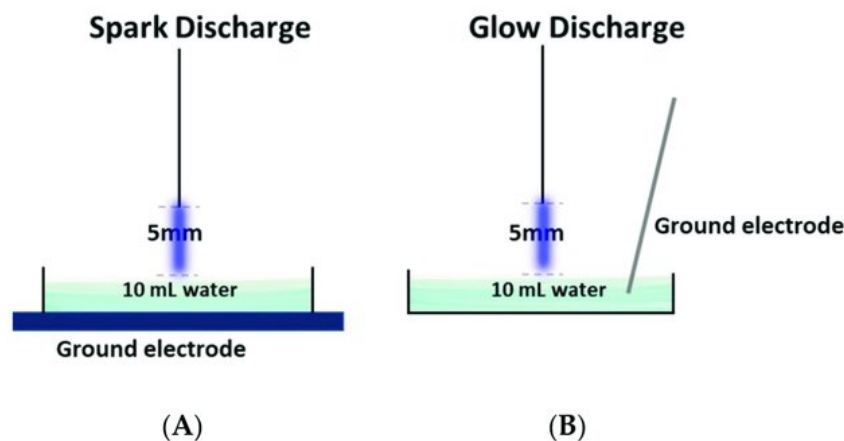


Figure 5. Schematic of air discharge in contact with water, (A) spark discharge, (B) glow discharge. Reprinted with permission from Ref. [100].

Roy et al. [69] introduce a unique DBD system over water in contact with the electrode for nitrogen fixation into NO_3 , which enables experiments to be carried out with a minimum electrode separation, overcoming the problem of water surface instability. A decrease in applied voltage and electrode spacing resulted in a promising energy cost for nitrogen fixation as low as 20.7 MJ/mol N. Increasing the applied voltage leads to higher production rates (up to 26 $\mu\text{mol}/\text{min}$) but also increases power absorption, reducing energy yield. Additionally, lower electrode gaps lead to a diffuse mode, which efficiently produces NO_3 . Packed bed DBD reactors, as shown in Figure 6, have also been investigated due to the promise of improving product selectivity and energy efficiency by performing the plasma reaction over a catalyst. The generation of NO_x in a DBD filled with several catalyst support materials ($\alpha\text{-Al}_2\text{O}_3$, $\gamma\text{-Al}_2\text{O}_3$, TiO_2 , MgO , TaTiO_3 , and quartz wool) was studied by Patil et al. [68]. A $\gamma\text{-Al}_2\text{O}_3$ catalyst with the lowest particle size of 250–160 nm produced the greatest results. However, the obtained energy cost was considerable (18 MJ/mol N), and the product yield was low (0.5 mol%) in comparison to comparable atmospheric pressure plasma reactors. Many metal oxides were deposited onto the support and assessed for their ability to produce NO_x with plasma assistance. The maximum concentration of NO_x was formed by the 5% $\text{WO}_3/\text{Al}_2\text{O}_3$ mixture, which was 10% more than that of the $\gamma\text{-Al}_2\text{O}_3$ alone. Selectivity toward NO fell despite an increase in NO_x content; this was explained by oxidation interactions with oxygen species on the catalyst surface. The extremely low electric field, more than 100–200 Td, which produces extremely energetic electrons and leads mainly to electronic excitation, ionization, and dissociation instead of vibrational excitation, may account for these subpar DBD results. This prevents the most energy-efficient NO_x formation pathway through the vibrationally induced Zeldovich mechanism [93]. Li et al. [70] used needle array electrodes in packed bed DBD reactors with $\alpha\text{-Al}_2\text{O}_3$ and $\gamma\text{-Al}_2\text{O}_3$ beads to improve NO_x formation at various discharge parameters and oxygen levels. The unfilled reactor and $\gamma\text{-Al}_2\text{O}_3$ PBR produced the highest NO_x concentrations (1.1% and 0.97%, respectively) at a low energy cost of 17 MJ/mol N and 33 MJ/mol N. The authors also demonstrated that increasing pulse width and repetition rate increases discharge power, resulting in higher electron density.

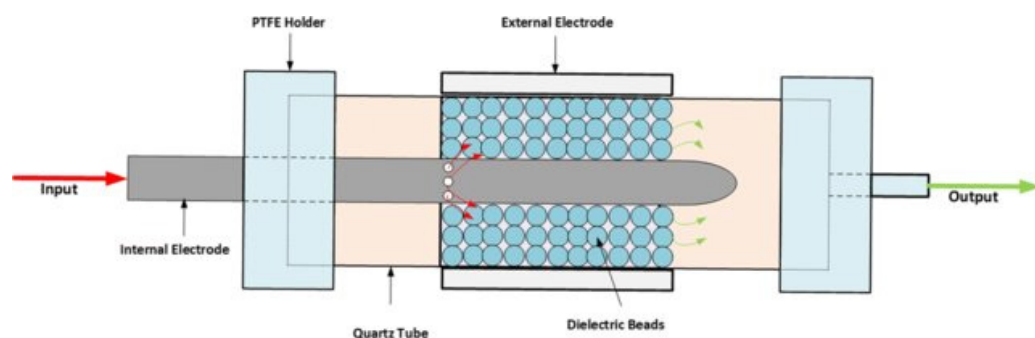


Figure 6. Packed DBD plasma reactor with a dielectric material. Reprinted with permission from Ref. [101].

Low-pressure MW plasmas produced the best outcomes in terms of energy consumption and product yield. For a NO concentration of 6 mol%, it was reported that a MW plasma with a catalyst used 0.84 MJ/mol N of energy. [54]. An electron cyclotron resonance plasma, which is a subset of magnetic field plasmas, yielded the highest NO concentration of 14% at the lowest energy cost of 0.28 MJ/mol N [80]. However, these results were published in the 1980s and have not been confirmed since. As a result, the claimed energy yield estimates for the 1980s MW plasma-based NO_x generation should be questioned. Low pressures (66 mbar) during the operation of these MW plasmas promote vibrational-translational nonequilibrium and, as a result, vibrational-induced Zeldovich mechanisms. This, therefore, contributes to the explanation of their excellent yields and low energy use. Nevertheless, low energy consumption only takes into consideration plasma power; they do not take into account the energy needed for the reactor cooling mechanism and the vacuum apparatus. Consequently, creating NO_x in a MW plasma would require more energy overall. MW reactors may also operate at higher pressures, but as collision frequency increases, heat losses increase. [102]. Kim et al. [79] reported 3.76 MJ/mol N and 0.6% NO_x in 2010 for an MW plasma slightly below atmospheric pressure, an input power between 60 and 90 W, and a fixed flow rate of 6 L/min. Power pulsing in a MW reactor may limit undesirable vibrational-translational relaxation, raising the vibrational temperature and, hence, the vibrational-translational non-equilibrium required for vibration-induced N₂ dissociation [103]. A diagram for a microwave plasma reactor is illustrated in Figure 7.

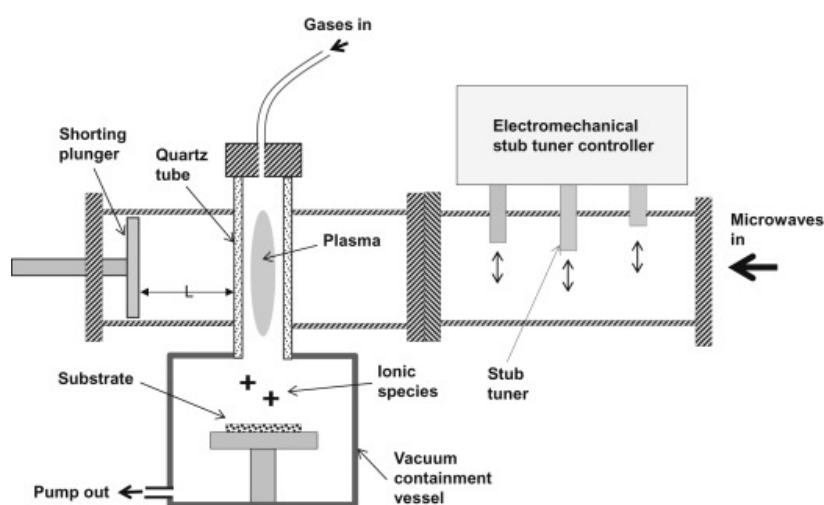


Figure 7. A waveguide-based microwave plasma reactor. Reprinted with permission from Ref. [104].

Pei et al. [59] assessed DBD, glow, spark, and arc-type plasmas, among others, and found an important feature that seemed to link the energy cost of NO_x production with a

broad range of discharges. As the authors have shown, NO_x generation efficiency may be greatly controlled by the average electric field and average gas temperature of the discharge. The effective electron-impact activation of N₂ molecules by an electric field to promote NO_x formation and the fast thermal quenching of NO to prevent its conversion back to N₂ and O₂ molecules when the gas temperature drops more slowly are the two main mechanisms that control the energy efficiency of NO_x production in any type of discharge. Strong electric fields cause N atoms to form, which is a crucial process for NO_x breakdown [74]. The authors proposed many strategies for lowering the average gas temperature, including cooling the reactor walls with water, utilizing short-duration high-current pulses, and prolonging the discharge length [56]. Vervloessem et al. [105] presented a pulsed plasma jet using dry air with an energy consumption of 0.42 MJ/mol N. The authors illustrated that pulsing is the main factor of the reactor's efficiency, as it decreases the temperature of the gas between the pulses, causing the Zeldovich mechanism's forward and reverse reaction rates to be delicately impacted. However, the NO_x concentrations obtained are very low at 0.02%, making this system unsuitable for practical applications.

NO_x formation by plasma jets flowing in (ambient) air (or N₂ atmosphere) and reacting with water has been observed [81–91]. While NH₃/NH₄⁺ creation was the main focus of this investigation, the presence of oxygen also led to the detection of NO₂ and NO₃ formation. Water and plasma jets work together to extract the NO_x product and stop the plasma from destroying it.

Process parameters, including gas composition, flow rate, and temperature, also play an important role in NO_x production, and their influence has been studied extensively. Lee et al. [106] investigated the influence of flow rate and oxygen content on NO_x generation by microwave plasma. A reduction in inlet flow rate from 45 standard liters per minute (slpm) to 25 slpm brought about a sharp rise in NO_x concentration from 1612 ppm to 9380 ppm when paired with an increase in O₂ content from 1% to 3%. The NO₂/NO ratio rose as the flow rate increased (from 4.3% to 14.8%). Na et al. [107] generated NO using a microwave plasma torch, and different N₂ (5–30 slpm) and O₂ (0–250 standard cubic centimeters per minute (sccm)) flow rates were examined. Abdelaziz et al. [108] investigated gas composition and residence time in a high-frequency spark discharge plasma as a factor of NO_x formation. The study has found that O₂ greatly affected the selectivity of NO_x products. 95% NO selectivity was reached with 5% O₂ and 43.8% NO₂ selectivity was found at 80% O₂. Altering the residence time improved the NO selectivity while maintaining a low energy consumption of 2.1 MJ/mol N. Li et al. [109] used a magnetic field stabilized plasma to investigate the correlation between gas temperature and electric field versus NO_x production. They have found that reducing these parameters increases NO_x production, resulting in an energy consumption of 2.29 MJ/mol N and a concentration of 15.925 ppm NO_x.

Patil et al. [73] conducted a detailed experimental analysis of the process parameters in gliding arc discharge reactors. In their study, oxygen concentrations ranging from 35 to 48% were determined to be ideal for NO_x generation, with NO selectivity decreasing linearly with increasing O₂ content until the O₂ concentration reached 48%. An increase in O₂ content had no noticeable effect on NO selectivity. It was also discovered in this study that the NO selectivity reduced as the feed flow rate increased. Lowering the flow rate was found to increase the specific energy intake and residence time of the reactant, resulting in a greater conversion of NO to NO₂. Furthermore, at the lowest flow rate of 0.5 L/min, the maximum NO_x concentration of 1.4% was achieved.

Temperature affects NO_x generation, according to Malik et al. [110], who used pulsed sliding discharge to assess the temperature effect on NO_x production. They found that when the electrode/dielectric surface in contact with the plasma was heated from 20 °C to 420 °C, the generation of NO rose while the production of ozone and NO₂ decreased. Additionally, it was found that at the same peak voltage, the energy per pulse increased. High temperatures have the potential to degrade ozone and impede the conversion of NO to NO₂. At 420 °C, the NO₂/NO ratio dropped to 0.25, and the energy required to produce

NO was 24–67 MJ/mol. Li et al. [111] noticed an opposite trend, with the NO_2/NO ratio slightly increasing from 0.67 at 273 K to 0.80 at 373 K in their corona discharge investigation. It should be emphasized that the gas temperature changes greatly depending on the type of plasma, reactor, and operation parameters used; therefore, the temperature effect should be evaluated alongside other aspects rather than independently. Furthermore, additional heating or cooling will raise the energy cost of NO_x production as well as the process's capital expenses.

Although plasma catalysis has been the subject of extensive research recently, relatively little has been published about NO_x production. Cavadias and Amouroux employed WO_3 as catalysts, which produced a nitrogen fixation rate of 19%, which is significantly greater than the rate reached using plasma alone under low pressure (8%) [43]. Their study was conducted at atmospheric pressure using a fluidized bed reactor, demonstrated in Figure 8, with a $\text{WO}_3/\text{Al}_2\text{O}_3$ catalyst [112].

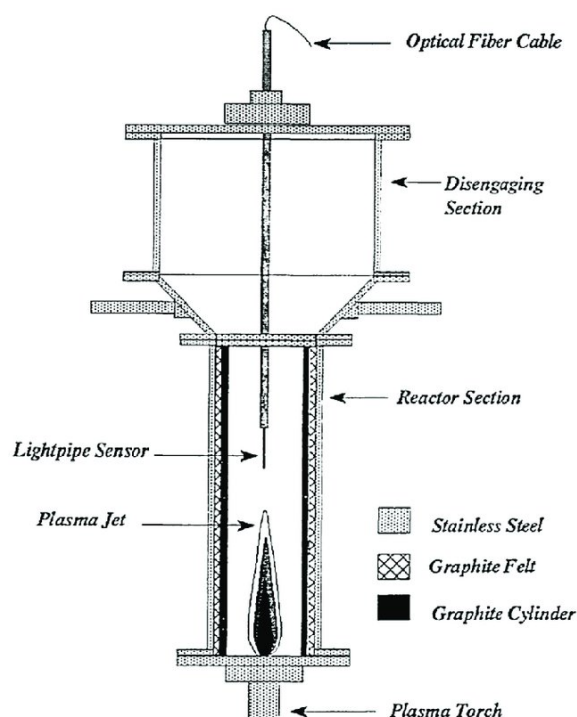


Figure 8. Representation of the fluid bed reactor. Reprinted with permission from Ref. [113].

Mattre, Amouroux, et al. studied the principles of the interaction between the solid catalyst surface and the chemical species that comprise plasma [43]. WO_3 and MoO_3 , two transition metal oxides, were used to study the plasma catalytic process. These catalytic substances were applied to large-surface-area supports, including ZrO_2 , MgO , and Al_2O_3 . N-type semiconductors are catalysts such as WO_3 and MoO_3 . These catalysts feature labile oxygen, which makes it easier to supply the oxygen needed for the oxidation of nitrogen to NO_x . This oxygen's lability may be crucial to the creation of NO_x . The oxidation process may go considerably more smoothly when a vibrationally stimulated N_2 molecule lands on a surface with labile oxygen [45,54,114]. In their investigations, Mutel et al. employed MoO_3 as catalysts and obtained an energy consumption of 28 MJ/kg of NO, which was 78% greater than that of a plasma jet arc generator [54]. Cu-ZSM-5 and Na-ZSM-5 catalytic activity was investigated by Sun et al. in a DBD reactor with pellets. Nonetheless, the study's primary goal was to investigate ideal processing circumstances for NO_x removal. Cu-ZSM-5 produced significantly more NO_x than Na-ZSM-5 when heated to 350 °C [115]. Pei et al. [116] have shed light on how activated Al_2O_3 catalysts may improve the energy efficiency of NO_x generation in air plasma jet and pin-pin DC glow discharge systems. Energy consumption can be significantly reduced by up to 45%

when the active Al_2O_3 is used in the DC glow discharge system, especially at 70 mA discharge current, at lower gas flow rates. The produced NO_2 is significantly increased by the activated Al_2O_3 catalyst, even though it is situated outside of the plasma zone. Additionally, the production of NO_2 by using an air plasma jet infused with floating activated Al_2O_3 powder was investigated. The utilization of a neodymium magnet ring effectively alleviated the occasional destabilization of the plasma discharge caused by the floating catalyst, which improved the homogeneity and stability of the plasma jet. At larger discharge currents, the energy efficiency was dramatically increased using the floating catalytic particle technique. With this method, the lowest energy cost for producing NO_2 was observed at 2.9 MJ/mol [116].

O'Hare [117,118] patented catalysts to produce NO. As stated by O'Hare, these catalysts also serve as a barrier to prevent the product from dissociating from UV radiation produced by electric excitation. According to the invented procedure, a more efficient discharge mechanism and higher/atmospheric pressure are possible. Catalytic materials described include WO_3 , MoO_3 , Ta_2O_5 , and other metal oxides adsorbed on Al_2O_3 , Fe_2O_3 , TiO_2 , SiO_2 , Na γ type zeolite, Ni γ type zeolite, Co γ type zeolite, and Mn χ and γ type zeolite. O'Hare outlines a technique in which low frequency, high voltage electric arc discharge and catalyst are combined, with the electric arc forming completely inside the catalyst bed. As catalysts, WO_3 , MgO , Ta_2O_5 , MoO_3 , Cr_2O_3 , $\text{Cu}_2\text{Cr}_2\text{O}_5$, and porous Al were employed. The suitability of each of these patented catalytic materials for the generation of plasma NO_x has not been properly examined. Using nano-sized TiO_2 photocatalysts in a three-level, coupled, rotating electrodes plasma was shown by Lei et al. [119] to increase the concentration of NO_x up to 8335 ppm and lowering the energy consumption from 2.91 MJ/mol N to 1.73 MJ/mol N. The authors claim that the TiO_2 catalyst is activated by oxygen species, which allows for the conductive band and valence band mechanism to proceed.

Using Pt, CuO, Fe, and Ag gauzes as catalysts, Belova et al. [120] studied the NO production reaction in a glow-discharge reactor. The 1:1 and 1:4 ratios of nitrogen to oxygen mixtures were used in the studies. With a NO of 9% for the 1:1 example, Pt was shown to give the highest nitrogen fixation rate in both circumstances. In ratios of 1:4, Pt may provide 7.25% of NO. The sequence of catalyst effectiveness for nitric oxide production is given as Pt > CuO > Cu > Fe > Ag [120]. Using seeding material could be an additional option. Alamaro [121] reports using seeding material to increase NO production efficiency. It was found that the collision rate increases noticeably with seeding, leading to a rise in the excitation and dissociation rates. Seeding is accomplished by reusing 5% of the mixture that exits the discharge. By 10% to 20% more NO was produced after seeding, resulting in a steady state concentration of 6% NO. Bayer et al. [122] investigated using a non-porous Ag wire catalyst in an RF plasma jet to improve NO formation. The authors found that the non-porous Ag wire catalyst improved the conversion rate of N to NO through mass transfer processes rather than surface reactions. The use of this type of catalyst is limited, however, to cases where diffusion transport to the catalyst surface is faster than the consumption of the reactive gases. Yu et al. [123] studied NO production optimization in a parallel-plate RF plasma with Fe and Pt catalysts over a SiO_2 support. They have found that the maximum production of NO was achieved at a conversion rate of 0.085%. The study showcased that the catalysts are non-reactive at room temperature, and NO is oxidized by O_3 to NO_2 and N_2O_5 ; however, at elevated temperatures, O_3 quickly decomposes, allowing higher NO_x yields.

Recent efforts to upscale plasma-based nitrogen fixation have been made. Tsonev et al. [92] investigated this challenge using two pin-to-pin DC plasma reactors—a small one operating up to 20 L/min and a larger one operating up to 300 L/min. The large reactor was also tested in torch configuration. For the small reactor, the authors were able to achieve an energy consumption of 2.8 MJ/mol N with a concentration of 1.72% NO_x or 4.8 MJ/mol N with a concentration of 3.51% NO_x . In the larger reactor, they were able to achieve 2.9 MJ/mol N with a concentration of 0.11% NO_x or 4.5 MJ/mol N with a concentration

of 0.21% NO_x in the pin-to-pin configuration; however, in the torch configuration, they achieved 2.9 MJ/mol N with a concentration of 0.31% NO_x. This study showcased how flow rates affect NO_x concentrations, thus affecting energy consumption, as well as how important reactor design is in upscaling systems.

3. Prospects of Nitrogen Fixation

When it comes to energy consumption and product production, considering that the H-B process has been refined for over a century, the plasma-assisted nitrogen fixation approach is still not comparable to it. As suggested by Patil et al., future studies ought to concentrate on energy consumption beneath 33–35 GJ/ton of N and production concentration exceeding 15% [18]. Additional research on plasma reactors and the relationship between plasma and catalysis is required to achieve this goal. The choice of catalysts is crucial in plasma catalysis for nitrogen fixation, and further study on catalyst screening will be required. Furthermore, numerous plasma procedures have demonstrated the advantages of pulsed energization [124–127]. The utilization of high-frequency nanosecond pulsing for plasma production can optimize both the yield and energy efficiency of the plasma-assisted nitrogen fixation process. The three main components for the energy performance of the plasma-assisted nitrogen fixation process are, according to Anastasopoulou et al. [128], the integration of renewable energy, the power supply system and reactor, and the process design at the industrial scale. Few studies have been conducted on topics such as product separation, absorption, or process design as a whole; much of the research conducted to date has been on the reactor itself. Moreover, creating large-scale plasma processes is a difficult task. Due to the complexity of plasma, only a relatively small amount of information has been discovered thus far to scale up nitrogen fixation processes that use plasma assistance. However, the industrialized plasma method, which uses scale-up approaches in the generation of ozone via multiple parallel reactors, provides valuable knowledge that could be gained [129,130].

Nonetheless, over the past few decades, technology for producing renewable energy has improved quickly. The high energy requirements of the plasma process might be substantially offset by integration with renewable energy, which would also offer a long-term solution to the environmental issues associated with industrial nitrogen fixation. The plasma plant might be powered by electricity produced by renewable energy sources like solar and wind. Furthermore, the idea of decentralized production is well fitted to the small-scale nature of the plasma-assisted nitrogen fixation process. Plants with container or modular sizes could be created for the small-scale synthesis of ammonia or NO_x for use in fuels and fertilizers. This will facilitate on-site production, give flexibility to meet fluctuating demand, and significantly save transportation costs and product loss. Even with the advancements over the last few decades and the increasing interest, plasma-assisted nitrogen fixation technology has a long way to go before it can compete with the H-B process on an industrial scale. On the contrary, it is anticipated that small-scale applications could become a reality soon enough, given certain circumstances. A decentralized method with plasma assistance can better suit the needs of low capital costs, scale-down economics, and localized usage of abundant renewable resources rather than large-scale industrial fertilizer production. Parallel to technological development, an assessment of the techno-economic viability and sustainability of the plasma-assisted nitrogen fixation process must be carried out [128,131,132]. This will provide suggestions for further improving process efficiency toward real applications.

4. Conclusions

The industrial imperative of nitrogen fixation is apparent in the face of global demands for nitrogen-containing compounds, ranging from fertilizers that sustain agriculture to pharmaceuticals, explosives, and pigments. However, the chemical inertness of molecular nitrogen demands a transformative process, nitrogen fixation, to turn it into reactive forms like ammonia or nitrates. Biological nitrogen fixation represents a natural and sustainable

pathway; its relatively slow speed poses challenges in meeting the escalating fertilizer requirements. The industrialization of nitrogen fixation, epitomized by the H-B process, has played a pivotal role in addressing this gap, enabling the exponential growth of global food production. However, the success of the H-B process comes at a significant cost, both in terms of energy intensity and environmental impact. As the H-B process approaches its theoretical energy efficiency limits, the process's reliance on fossil fuels and the release of substantial greenhouse gas emissions underscores the need for more sustainable alternatives. Plasma nitrogen fixation processes present advantages such as utilizing abundant materials like air and water, as well as the potential for renewable energy sources. While the energy efficiency of plasma-assisted nitrogen fixation is yet to match that of the H-B process, ongoing research and technological advancements offer promising avenues for improvement. The reaction mechanism of NO_x formation follows the Zeldovich mechanism. Researchers have investigated and documented the conversion of atmospheric nitrogen fixation into NO_x for laboratory-scale procedures utilizing air plasma. Various plasma reactors have been examined for NO_x production, including spark discharges, glow discharges, corona discharges, laser-produced discharges, radio-frequency crossed discharges, dielectric barrier discharges, arc discharges, microwave discharges, and plasma jets in contact with water. Research demonstrated that by optimizing the reactor and avoiding the transmission of vibrational energy from N_2 to O_2 , energy consumption could be reduced to 0.5 MJ/mol N. Studies have shown that in a variety of discharges, the average electric field and the average gas temperature of the discharge, the influence of flow rate, and oxygen content can largely regulate NO_x generation efficiency. Employing catalysts to plasma significantly increased the rate of NO_x generation compared to plasma alone under low pressure. Catalysts aid in the supply of oxygen needed for the oxidation of nitrogen to NO_x , as well as serve as a barrier to prevent the product from dissociating from UV radiation produced by electric excitation. The integration of renewable energy, the power supply system and reactor, and the process design at the industrial scale are the three primary components of the energy performance of the plasma-assisted nitrogen fixation process. Renewable energy technology has advanced rapidly during the last few decades. The plasma process's high energy requirements could be significantly compensated by integration with renewable energy, which would also provide a long-term solution to the environmental difficulties connected with industrial nitrogen fixation. Furthermore, the concept of decentralized production fits the small-scale character of the plasma-assisted nitrogen fixation process perfectly. Plants with modular sizes could be developed for small-scale ammonia or NO_x production for fuel and fertilizer use. This will allow for on-site production, flexibility to meet variable demand, and a considerable reduction in transportation costs and product waste.

Author Contributions: Writing—original draft preparation, A.K.; writing—review and editing, A.K. and D.G.P. All authors have read and agreed to the published version of the manuscript.

Funding: This research received no external funding.

Data Availability Statement: No new data were created or analyzed in this study. Data sharing does not apply to this article.

Acknowledgments: We thank the grant from the Army Research Office (ARO), Army Research Laboratory (ARL), the Office of Naval Research (ONR), and Purdue University for the support of our lab. Additional thanks to the Army Research Office under Cooperative Agreement Number W911NF-22-2-0170 for funding Angeliqe Klimek's Ph.D. The views and conclusions contained in this document are those of the authors and should not be interpreted as representing the official policies, either expressed or implied, of the Army Research Office or the U.S. Government.

Conflicts of Interest: The authors declare no conflicts of interest.

References

1. Wagner, S.C. Biological Nitrogen Fixation. Nature Education Knowledge, 3, 15.—References—Scientific Research Publishing. 2011. Available online: <https://www.scirp.org/reference/referencespapers?referenceid=1323846> (accessed on 8 May 2023).
2. Erisman, J.W.; Galloway, J.N.; Dise, N.B.; Sutton, M.A.; Bleeker, A.; Grizzetti, B.; Leach, A.M.; de Vries, W. *Nitrogen: Too Much of a Vital Resource: Science Brief*; WWF Netherlands: Zeist, The Netherlands, 2015.
3. Galloway, J.N.; Cowling, E.B. Reactive Nitrogen and the World: 200 Years of Change. *AMBIO A J. Hum. Environ.* **2002**, *31*, 64–71. [[CrossRef](#)] [[PubMed](#)]
4. Bernhard, A. The Nitrogen Cycle: Processes, Players, and Human Impact. Available online: <https://www.nature.com/scitable/knowledge/library/the-nitrogen-cycle-processes-players-and-human-15644632/> (accessed on 8 May 2023).
5. Klopsch, I.; Yuzik-Klimova, E.Y.; Schneider, S. Functionalization of N₂ by Mid to Late Transition Metals via N–N Bond Cleavage. *Nitrogen Fixat.* **2017**, 71–112. [[CrossRef](#)]
6. Jiang, J.; He, X.; Li, L.; Li, J.; Shao, H.; Xu, Q.; Ye, R.; Dong, Y. Effect of Cold Plasma Treatment on Seed Germination and Growth of Wheat. *Plasma Sci. Technol.* **2014**, *16*, 54–58. [[CrossRef](#)]
7. Erisman, J.W.; Sutton, M.A.; Galloway, J.; Klimont, Z.; Winiwarter, W. How a Century of Ammonia Synthesis Changed the World. *Nat. Geosci.* **2008**, *1*, 636–639. [[CrossRef](#)]
8. Galloway, J.N.; Townsend, A.R.; Erisman, J.W.; Bekunda, M.; Cai, Z.; Freney, J.R.; Martinelli, L.A.; Seitzinger, S.P.; Sutton, M.A. Transformation of the Nitrogen Cycle: Recent Trends, Questions, and Potential Solutions. *Science* **2008**, *320*, 889–892. [[CrossRef](#)] [[PubMed](#)]
9. Bezdek, M.J.; Chirik, P.J. Expanding Boundaries: N₂ Cleavage and Functionalization beyond Early Transition Metals. *Angew. Chem. Int. Ed.* **2016**, *55*, 7892–7896. [[CrossRef](#)] [[PubMed](#)]
10. Smil, V. *Enriching the Earth: Fritz Haber, Carl Bosch, and the Transformation of World Food Production*; MIT Press: Cambridge, UK, 2004.
11. Smil, V. Nitrogen and Food Production: Proteins for Human Diets. *AMBIO A J. Hum. Environ.* **2002**, *31*, 126–131. [[CrossRef](#)] [[PubMed](#)]
12. World Population Prospects: The 2017 Revision. UN DESA Publications. Available online: <https://desapublications.un.org/publications/world-population-prospects-2017-revision> (accessed on 8 May 2023).
13. Travis, A.S.; Springerlink (Online Service). *Nitrogen Capture: The Growth of an International Industry (1900–1940)*; Springer International Publishing: Cham, Switzerland, 2018.
14. Tamaru, K. *The History of the Development of Ammonia Synthesis*; Springer: Boston, MA, USA, 1991; pp. 1–18. [[CrossRef](#)]
15. Travis, A.S. Electric Arcs, Cyanamide, Carl Bosch and Fritz Haber. In *SpringerBriefs in Molecular Science*; Springer: Cham, Switzerland, 2015; pp. 17–72. [[CrossRef](#)]
16. Leigh, G.J. *Nitrogen Fixation at the Millennium*; Elsevier: Amsterdam, The Netherlands, 2002.
17. Ernst, F.A. *Fixation of Atmospheric Nitrogen*; D. Van Nostrand Company: New York, NY, USA, 1928.
18. Patil, B.S.; Wang, Q.; Hessel, V.; Lang, J. Plasma N₂-Fixation: 1900–2014. *Catal. Today* **2015**, *256*, 49–66. [[CrossRef](#)]
19. The Haber-Bosch Heritage: The Ammonia Production Technology. Fertilizer. Available online: <https://www.fertilizer.org/resource/the-haber-bosch-heritage-the-ammonia-production-technology> (accessed on 8 May 2023).
20. Cherkasov, N.; Ibhaddon, A.O.; Fitzpatrick, P. A Review of the Existing and Alternative Methods for Greener Nitrogen Fixation. *Chem. Eng. Process. Process Intensif.* **2015**, *90*, 24–33. [[CrossRef](#)]
21. Vu, M.-H.; Sakar, M.; Do, T.-O. Insights into the Recent Progress and Advanced Materials for Photocatalytic Nitrogen Fixation for Ammonia (NH₃) Production. *Catalysts* **2018**, *8*, 621. [[CrossRef](#)]
22. Schrock, R.R. Reduction of Dinitrogen. *Proc. Natl. Acad. Sci. USA* **2006**, *103*, 17087. [[CrossRef](#)] [[PubMed](#)]
23. Tanabe, Y.; Nishibayashi, Y. Developing More Sustainable Processes for Ammonia Synthesis. *Coord. Chem. Rev.* **2013**, *257*, 2551–2564. [[CrossRef](#)]
24. Pfromm, P.H. Towards Sustainable Agriculture: Fossil-Free Ammonia. *J. Renew. Sustain. Energy* **2017**, *9*, 034702. [[CrossRef](#)]
25. Barbir, F. PEM Electrolysis for Production of Hydrogen from Renewable Energy Sources. *Sol. Energy* **2005**, *78*, 661–669. [[CrossRef](#)]
26. Egeland, A.; Burke, W.J.; Springerlink (Online Service). *Kristian Birkeland: The First Space Scientist*; Springer: Dordrecht, The Netherlands; New York, NY, USA, 2005.
27. Fridman, A.A. *Plasma Chemistry*; Cambridge University Press: Cambridge, UK, 2012.
28. Lieberman, M.A.; Lichtenberg, A.J. *Principles of Plasma Discharges and Materials Processing*; John Wiley & Sons: New Jersey, NJ, USA, 2005.
29. Fauchais, P.; Rakowitz, J. Physics on Plasma Chemistry. *J. Phys. Colloq.* **1979**, *40*, C7-289–C7-312. [[CrossRef](#)]
30. Hippler, R.; Pfau, S.; Schmidt, M.; Schoenbach, K.H. *Low Temperature Plasma Physics*; Wiley-VCH: Weinheim, Germany, 2001.
31. Birkeland, K. On the Oxidation of Atmospheric Nitrogen in Electric Arcs. *Trans. Faraday Soc.* **1906**, *2*, 98. [[CrossRef](#)]
32. Eyde, S. Oxidation of Atmospheric Nitrogen and Development of Resulting Industries in Norway. *J. Ind. Eng. Chem.* **1912**, *4*, 771–774. [[CrossRef](#)]
33. Eremin, E.N.; Maltsev, A.N. Thermodynamic equilibrium concentrations of nitrogen oxide. *Russ. J. Phys. Chem.* **1956**, *30*, 1179–1181.
34. International Energy Agency. World Energy Outlook 2020—Analysis. IEA. Available online: <https://www.iea.org/reports/world-energy-outlook-2020> (accessed on 29 December 2023).

35. Rusanov, V.D.; Fridman, A.A.; Sholin, G.V. The Physics of a Chemically Active Plasma with Nonequilibrium Vibrational Excitation of Molecules. *Sov. Phys. Uspekhi* **1981**, *24*, 447–474. [[CrossRef](#)]
36. Rusanov, V.D.; Fridman, A.A.; Sholin, G.V. Nitrogen Oxide Synthesis in nonequilibrium Plasma Chemical Systems, Ed. *Smirnov Smirnov BM "At." Mosc.* **1978**, *5*, 222–240.
37. Li, S.; Medrano Jimenez, J.; Hessel, V.; Gallucci, F. Recent Progress of Plasma-Assisted Nitrogen Fixation Research: A Review. *Processes* **2018**, *6*, 248. [[CrossRef](#)]
38. Lamichhane, P.; Paneru, R.; Nguyen, L.N.; Lim, J.S.; Bhartiya, P.; Adhikari, B.C.; Mumtaz, S.; Choi, E.H. Plasma-Assisted Nitrogen Fixation in Water with Various Metals. *React. Chem. Eng.* **2020**, *5*, 2053–2057. [[CrossRef](#)]
39. Winter, L.R.; Chen, J.G. N₂ Fixation by Plasma-Activated Processes. *Joule* **2021**, *5*, 300–315. [[CrossRef](#)]
40. Chen, H.; Yuan, D.; Wu, A.; Lin, X.; Li, X. Review of Low-Temperature Plasma Nitrogen Fixation Technology. *Waste Dispos. Sustain. Energy* **2021**, *3*, 201–217. [[CrossRef](#)] [[PubMed](#)]
41. Huang, Z.; Xiao, A.; Liu, D.; Lu, X.; Ostrikov, K. Plasma-Water-Based Nitrogen Fixation: Status, Mechanisms, and Opportunities. *Plasma Process. Polym.* **2022**, *19*, 2100198. [[CrossRef](#)]
42. Frost, D.C.; McDowell, C.A. The Dissociation Energy of the Nitrogen Molecule. Proceedings of the Royal Society of London. Series A. *Math. Phys. Sci.* **1956**, *236*, 278–284. [[CrossRef](#)]
43. Rapakoulias, D.; Amouroux, J. Processus Catalytiques Dans Un Réacteur à Plasma Hors d'Équilibre II. Fixation de l'Azote Dans Le Système N₂-O₂. *Rev. Phys. Appl.* **1980**, *15*, 1261–1265. [[CrossRef](#)]
44. Rapakoulias, D.; Amouroux, J. Réacteur de Synthèse et de Trempe Dans Un Plasma Hors d'Équilibre: Application à La Synthèse de C₂H₂ et HCN. *Rev. Phys. Appl.* **1979**, *14*, 961. [[CrossRef](#)]
45. Cavadias, S.; Amouroux, J. Synthesis of nitrogen oxides in plasma reactors. *Bull. Soc. Chim. Fr.* **1986**, *2*, 147–158.
46. Pollo, I.; Hoffmann-Fedenczuk, K.; Fedenczuk, L. The influence of gas-inlet and quenching systems on the nitrogen oxides production in air plasmas. *Int. Symp. Plasma Chem.* **1981**, *2*, 756–760.
47. Pollo, I.; Banasik, S. Experiments on the synthesis of nitric oxide in an argon plasma. *Chem. Plazmy* **1978**, 259–270.
48. Krop, J.; Pollo, I. Chemical reactors for synthesis of nitrogen oxide in a stream of low-temperature plasma. III. Reactor to freeze reaction products by injection of water. *Chemia* **1981**, *678*, 51–59.
49. Krop, J.; Pollo, I. Chemical reactors for synthesis of nitrogen oxide in low temperature of air plasma jet. II, Efficiency of nitrogen oxide synthesis in reactors with rotating disk. *Chemia* **1980**, *633*, 25–33.
50. Krop, J.; Krop, E.; Pollo, I. Calculated amounts of nitric oxide in a nitrogen–oxygen plasma jet. *Chem. Plazmy* **1979**, 242–249.
51. Amouroux, J.; Cavadias, S.; Rapakoulias, D. Réacteur de Synthèse et de Trempe Dans Un Plasma Hors d'Équilibre: Application à La Synthèse Des Oxydes D'azote. *Rev. Phys. Appl.* **1979**, *14*, 969–976. [[CrossRef](#)]
52. Production of Nitric Monoxide in Dry Air Using Pulsed Discharge. IEEE Conference Publication. IEEE Xplore. Available online: <https://ieeexplore.ieee.org/document/823768> (accessed on 21 June 2023).
53. Production of Nitric Oxide Using a Pulsed Arc Discharge. IEEE Journals & Magazine. IEEE Xplore. Available online: <https://ieeexplore.ieee.org/document/1178015> (accessed on 21 June 2023).
54. Mutel, B.; Dessaux, O.; Goudmand, P. Energy Cost Improvement of the Nitrogen Oxides Synthesis in a Low Pressure Plasma. *Rev. Phys. Appl.* **1984**, *19*, 461–464. [[CrossRef](#)]
55. Pollo, I.; Banasik, S. Some problems of energy utilization in a plasma reactor with a direct current argon plasma generator. *Chemia* **1979**, *631*, 377–378.
56. Jardali, F.; Van Alphen, S.; Creel, J.; Ahmadi Eshtehardi, H.; Axelsson, M.; Ingels, R.; Snyders, R.; Bogaerts, A. NO_x Production in a Rotating Gliding Arc Plasma: Potential Avenue for Sustainable Nitrogen Fixation. *Green Chem.* **2021**, *23*, 1748–1757. [[CrossRef](#)]
57. Rouwenhorst, K.H.R.; Jardali, F.; Bogaerts, A.; Lefferts, L. From the Birkeland–Eyde Process towards Energy-Efficient Plasma-Based NO_x Synthesis: A Techno-Economic Analysis. *Energy Environ. Sci.* **2021**, *14*, 2520–2534. [[CrossRef](#)]
58. Rehbein, N.; Cooray, V. NO_x Production in Spark and Corona Discharges. *J. Electrostat.* **2001**, *51*, 333–339. [[CrossRef](#)]
59. Pei, X.; Gidon, D.; Yang, Y.-J.; Xiong, Z.; Graves, D.B. Reducing Energy Cost of NO Production in Air Plasmas. *Chem. Eng. J.* **2019**, *362*, 217–228. [[CrossRef](#)]
60. Janda, M.; Martišovitéš, V.; Hensel, K.; Machala, Z. Generation of Antimicrobial NO_x by Atmospheric Air Transient Spark Discharge. *Plasma Chem. Plasma Process.* **2016**, *36*, 767–781. [[CrossRef](#)]
61. Pavlovich, M.J.; Ono, T.; Galleher, C.; Curtis, B.; Clark, D.S.; Machala, Z.; Graves, D.B. Air Spark-like Plasma Source for Antimicrobial NO_x Generation. *J. Phys. D Appl. Phys.* **2014**, *47*, 505202. [[CrossRef](#)]
62. Abdelaziz, A.A.; Teramoto, Y.; Nozaki, T.; Kim, H.-H. Toward Reducing the Energy Cost of NO_x Formation in a Spark Discharge Reactor through Pinpointing Its Mechanism. *ACS Sustain. Chem. Eng.* **2023**, *11*, 4106–4118. [[CrossRef](#)]
63. Zhang, S.; Zong, L.; Zeng, X.; Zhou, R.; Liu, Y.; Zhang, C.; Pan, J.; Cullen, P.J.; Ostrikov, K.; Shao, T. Sustainable Nitrogen Fixation with Nanosecond Pulsed Spark Discharges: Insights into Free-Radical-Chain Reactions. *Green Chem.* **2022**, *24*, 1534–1544. [[CrossRef](#)]
64. Pei, X.; Gidon, D.; Graves, D.B. Specific energy cost for nitrogen fixation as NO_x using DC glow discharge in air. *J. Phys. D Appl. Phys.* **2019**, *53*, 044002. [[CrossRef](#)]
65. Nitrogen Fixation into Water by Pulsed High-Voltage Discharge. IEEE Journals & Magazine. IEEE Xplore. Available online: <https://ieeexplore.ieee.org/document/4735609> (accessed on 14 October 2023).

66. Rahman, M.; Cooray, V. NO_x Generation in Laser-Produced Plasma in Air as a Function of Dissipated Energy. *Opt. Laser Technol.* **2003**, *35*, 543–546. [[CrossRef](#)]
67. Partridge, W.S.; Parlin, R.B.; Zwolinski, B.J. Fixation of Nitrogen in a Crossed Discharge. *Ind. Eng. Chem.* **1954**, *46*, 1468–1471. [[CrossRef](#)]
68. Patil, B.S.; Cherkasov, N.; Lang, J.; Ibhaddon, A.O.; Hessel, V.; Wang, Q. Low Temperature Plasma-Catalytic NO_x Synthesis in a Packed DBD Reactor: Effect of Support Materials and Supported Active Metal Oxides. *Appl. Catal. B Environ.* **2016**, *194*, 123–133. [[CrossRef](#)]
69. Roy, N.C.; Maira, N.; Pattyn, C.; Remy, A.; Delplancke, M.-P.; Reniers, F. Mechanisms of Reducing Energy Costs for Nitrogen Fixation Using Air-Based Atmospheric DBD Plasmas over Water in Contact with the Electrode. *Chem. Eng. J.* **2023**, *461*, 141844. [[CrossRef](#)]
70. Li, Y.; Qin, L.; Wang, H.-L.; Li, S.-S.; Yuan, H.; Yang, D.-Z. High Efficiency NO_x Synthesis and Regulation Using Dielectric Barrier Discharge in the Needle Array Packed Bed Reactor. *Chem. Eng. J.* **2023**, *461*, 141922. [[CrossRef](#)]
71. Vervloessem, E.; Aghaei, M.; Jardali, F.; Hafezkhiani, N.; Bogaerts, A. Plasma-Based N₂ Fixation into NO_x: Insights from Modeling toward Optimum Yields and Energy Costs in a Gliding Arc Plasmatron. *ACS Sustain. Chem. Eng.* **2020**, *8*, 9711–9720. [[CrossRef](#)]
72. Coudert, J.; Bourdin, E.; Baronnet, J.-M.; Rakowitz, J.; Fauchais, P. Chemical kinetics study of nitrogen oxide synthesis in a DC plasma jet: A proposed model. *J. Physique. Colloq.* **1979**, *40*, C7-355–C7-356. [[CrossRef](#)]
73. Patil, B.S.; Peeters, F.J.J.; van Rooij, G.J.; Medrano, J.A.; Gallucci, F.; Lang, J.; Wang, Q.; Hessel, V. Plasma Assisted Nitrogen Oxide Production from Air: Using Pulsed Powered Gliding Arc Reactor for a Containerized Plant. *AIChE J.* **2017**, *64*, 526–537. [[CrossRef](#)]
74. Wang, W.; Patil, B.; Heijkers, S.; Hessel, V.; Bogaerts, A. Nitrogen Fixation by Gliding Arc Plasma: Better Insight by Chemical Kinetics Modelling. *ChemSusChem* **2017**, *10*, 2145–2157. [[CrossRef](#)] [[PubMed](#)]
75. Tsonev, I.; O'Modhrain, C.; Bogaerts, A.; Gorbanev, Y. Nitrogen Fixation by an Arc Plasma at Elevated Pressure to Increase the Energy Efficiency and Production Rate of NO_x. *ACS Sustain. Chem. Eng.* **2023**, *11*, 1888–1897. [[CrossRef](#)]
76. Muzammil, I.; Lee, D.H.; Dinh, D.K.; Kang, H.; Roh, S.A.; Kim, Y.N.; Choi, S.; Jung, C.; Song, Y.-H. A Novel Energy Efficient Path for Nitrogen Fixation Using a Non-Thermal Arc. *RSC Adv.* **2021**, *11*, 12729–12738. [[CrossRef](#)] [[PubMed](#)]
77. Chen, H.; Wu, A.; Mathieu, S.; Gao, P.; Li, X.; Xu, B.Z.; Yan, J.; Tu, X. Highly Efficient Nitrogen Fixation Enabled by an Atmospheric Pressure Rotating Gliding Arc. *Plasma Process. Polym.* **2021**, *18*, 2000200. [[CrossRef](#)]
78. Van Alphen, S.; Eshtehardi, H.A.; O'Modhrain, C.; Bogaerts, J.; Van Poyer, H.; Creel, J.; Delplancke, M.P.; Snyders, R.; Bogaerts, A. Effusion Nozzle for Energy-Efficient NO_x Production in a Rotating Gliding Arc Plasma Reactor. *Chem. Eng. J.* **2022**, *443*, 136529. [[CrossRef](#)]
79. Kim, T.; Song, S.; Kim, J.; Iwasaki, R. Formation of NO_x from Air and N₂/O₂ Mixtures Using a Nonthermal Microwave Plasma System. *Jpn. J. Appl. Phys.* **2010**, *49*, 126201. [[CrossRef](#)]
80. Asisov, R.I.; Givotov, V.K.; Rusanov, V.D.; Fridman, A. High energy chemistry (Khimia Vysokikh energij). *Sov. Phys.* **1980**, *14*, 366.
81. Peng, P.; Chen, P.; Addy, M.; Cheng, Y.; Zhang, Y.; Anderson, E.; Zhou, N.; Schiappacasse, C.; Hatzenbeller, R.; Fan, L.; et al. In Situ Plasma-Assisted Atmospheric Nitrogen Fixation Using Water and Spray-Type Jet Plasma. *Chem. Commun.* **2018**, *54*, 2886–2889. [[CrossRef](#)] [[PubMed](#)]
82. Gorbanev, Y.; Vervloessem, E.; Nikiforov, A.; Bogaerts, A. Nitrogen Fixation with Water Vapor by Nonequilibrium Plasma: Toward Sustainable Ammonia Production. *ACS Sustain. Chem. Eng.* **2020**, *8*, 2996–3004. [[CrossRef](#)]
83. Toth, J.R.; Abuyazid, N.H.; Lacks, D.J.; Renner, J.N.; Mohan Sankaran, R. A Plasma-Water Droplet Reactor for Process-Intensified, Continuous Nitrogen Fixation at Atmospheric Pressure. *ACS Sustain. Chem. Eng.* **2020**, *8*, 14845. [[CrossRef](#)]
84. Peng, P.; Schiappacasse, C.; Zhou, N.; Addy, M.; Cheng, Y.; Zhang, Y.; Anderson, E.; Chen, D.; Wang, Y.; Liu, Y.; et al. Plasma in Situ Gas–Liquid Nitrogen Fixation Using Concentrated High-Intensity Electric Field. *J. Phys. D Appl. Phys.* **2019**, *52*, 494001. [[CrossRef](#)]
85. Kubota, Y.; Kogo, K.; Ohno, M.; Hara, T. Synthesis of Ammonia through Direct Chemical Reactions between an Atmospheric Nitrogen Plasma Jet and a Liquid. *Plasma Fusion Res.* **2010**, *5*, 042. [[CrossRef](#)]
86. Kumari, S.; Pishgar, S.; Schwarting, M.E.; Paxton, W.F.; Spurgeon, J.M. Synergistic Plasma-Assisted Electrochemical Reduction of Nitrogen to Ammonia. *Chem. Commun.* **2018**, *54*, 13347–13350. [[CrossRef](#)] [[PubMed](#)]
87. Hawtof, R.; Ghosh, S.; Guarr, E.; Xu, C.; Mohan Sankaran, R.; Renner, J.N. Catalyst-Free, Highly Selective Synthesis of Ammonia from Nitrogen and Water by a Plasma Electrolytic System. *Sci. Adv.* **2019**, *5*, eaat5778. [[CrossRef](#)] [[PubMed](#)]
88. Haruyama, T.; Namise, T.; Shimoshimizu, N.; Uemura, S.; Takatsuji, Y.; Hino, M.; Yamasaki, R.; Kamachi, T.; Kohno, M. Non-Catalyzed One-Step Synthesis of Ammonia from Atmospheric Air and Water. *Green Chem.* **2016**, *18*, 4536–4541. [[CrossRef](#)]
89. Sakakura, T.; Uemura, S.; Hino, M.; Kiyomatsu, S.; Takatsuji, Y.; Yamasaki, R.; Morimoto, M.; Haruyama, T. Excitation of H₂O at the plasma/water interface by UV irradiation for the elevation of ammonia production. *Green Chem.* **2017**, *20*, 627–633. [[CrossRef](#)]
90. Sakakura, T.; Murakami, N.; Takatsuji, Y.; Morimoto, M.; Haruyama, T. Contribution of Discharge Excited Atomic N, N₂^{*}, and N₂⁺ to a Plasma/Liquid Interfacial Reaction as Suggested by Quantitative Analysis. *Chemphyschem* **2019**, *20*, 1467–1474. [[CrossRef](#)]
91. Sakakura, T.; Murakami, N.; Takatsuji, Y.; Haruyama, T. Nitrogen Fixation in a Plasma/Liquid Interfacial Reaction and Its Switching between Reduction and Oxidation. *J. Phys. Chem. C* **2020**, *124*, 9401–9408. [[CrossRef](#)]
92. Tsonev, I.; Ahmadi Eshtehardi, H.; Delplancke, M.-P.; Bogaerts, A. Scaling Up Energy-Efficient Plasma-Based Nitrogen Fixation. *Soc. Sci. Res. Netw.* **2023**. [[CrossRef](#)]

93. Bogaerts, A.; Neyts, E.C. Plasma Technology: An Emerging Technology for Energy Storage. *ACS Energy Lett.* **2018**, *3*, 1013–1027. [[CrossRef](#)]
94. Czernichowski, A. Gliding arc: Applications to engineering and environment control. *Pure Appl. Chem.* **1994**, *66*, 1301–1310. [[CrossRef](#)]
95. Ramakers, M.; Trenchev, G.; Heijkers, S.; Wang, W.; Bogaerts, A. Gliding Arc Plasmatron: Providing an Alternative Method for Carbon Dioxide Conversion. *ChemSusChem* **2017**, *10*, 2642–2652. [[CrossRef](#)] [[PubMed](#)]
96. Cleiren, E.; Heijkers, S.; Ramakers, M.; Bogaerts, A. Dry Reforming of Methane in a Gliding Arc Plasmatron: Towards a Better Understanding of the Plasma Chemistry. *ChemSusChem* **2017**, *10*, 4025–4036. [[CrossRef](#)]
97. Mousavi, S.A.; Piavis, W.; Turn, S. Reforming of biogas using a non-thermal, gliding-arc, plasma in reverse vortex flow and fate of hydrogen sulfide contaminants. *Fuel Process. Technol.* **2019**, *193*, 378–391. [[CrossRef](#)]
98. Janda, M.; Martišovič, V.; Hensel, K.; Dvonč, L.; Machala, Z. Measurement of the Electron Density in Transient Spark Discharge. *Plasma Sources Sci. Technol.* **2014**, *23*, 065016. [[CrossRef](#)]
99. Janda, M.; Hoder, T.; Sarani, A.; Brandenburg, R.; Machala, Z. Cross-Correlation Spectroscopy Study of the Transient Spark Discharge in Atmospheric Pressure Air. *Plasma Sources Sci. Technol.* **2017**, *26*, 055010. [[CrossRef](#)]
100. Tsoukou, E.; Delit, M.; Treint, L.; Bourke, P.; Boehm, D. Distinct Chemistries Define the Diverse Biological Effects of Plasma Activated Water Generated with Spark and Glow Plasma Discharges. *Appl. Sci.* **2021**, *11*, 1178. [[CrossRef](#)]
101. Mansouri, F.; Khavanin, A.; Jafari, A.J.; Asilian, H.; Ghomi, H.R.; Mousavi, S.M. Energy efficiency improvement in nitric oxide reduction by packed DBD plasma: Optimization and modeling using response surface methodology (RSM). *Environ. Sci. Pollut. Res.* **2020**, *27*, 16100–16109. [[CrossRef](#)]
102. Bruggeman, P.; Iza, F.; Brandenburg, R. Foundations of Atmospheric Pressure Non-Equilibrium Plasmas. *Plasma Sources Sci. Technol.* **2017**, *26*, 123002. [[CrossRef](#)]
103. van Alphen, S.; Vermeiren, V.; Butterworth, T.D.; van den Bekerom, D.C.; van Rooij, G.J.; Bogaerts, A. Power Pulsing to Maximize Vibrational Excitation Efficiency in N₂ Microwave Plasma: A Combined Experimental and Computational Study. *J. Phys. Chem. C* **2019**, *124*, 1765–1779. [[CrossRef](#)]
104. Mehdizadeh, M. *Plasma Applicators at RF and Microwave Frequencies*; William Andrew Publishers: Norwich, NY, USA, 2015; pp. 335–363. [[CrossRef](#)]
105. Vervloessem, E.; Gorbanev, Y.; Nikiforov, A.; Geyter, N.D.; Bogaerts, A. Sustainable NO_x Production from Air in Pulsed Plasma: Elucidating the Chemistry behind the Low Energy Consumption. *Green Chem.* **2022**, *24*, 916–929. [[CrossRef](#)]
106. Lee, J.; Sun, H.; Im, S.-K.; Bak, M.S. Formation of nitrogen oxides from atmospheric electrodeless microwave plasmas in nitrogen–oxygen mixtures. *J. Appl. Phys.* **2017**, *122*, 083303. [[CrossRef](#)]
107. Na, Y.H.; Kumar, N.; Kang, M.-H.; Cho, G.S.; Choi, E.H.; Park, G.; Uhm, H.S. Production of nitric oxide using a microwave plasma torch and its application to fungal cell differentiation. *J. Phys. D Appl. Phys.* **2015**, *48*, 195401. [[CrossRef](#)]
108. Abdelaziz, A.A.; Teramoto, Y.; Nozaki, T.; Kim, H.-H. Performance of High-Frequency Spark Discharge for Efficient NO Production with Tunable Selectivity. *Chem. Eng. J.* **2023**, *470*, 144182. [[CrossRef](#)]
109. Li, Z.; Wu, E.; Nie, L.; Liu, D.; Lu, X. Magnetic Field Stabilized Atmospheric Pressure Plasma Nitrogen Fixation: Effect of Electric Field and Gas Temperature. *Phys. Plasmas* **2023**, *30*, 083502. [[CrossRef](#)]
110. Malik, M.A.; Jiang, C.; Heller, R.; Lane, J.; Hughes, D.; Schoenbach, K.H. Ozone-Free Nitric Oxide Production Using an Atmospheric Pressure Surface Discharge—a Way to Minimize Nitrogen Dioxide Co-Production. *Chem. Eng. J.* **2016**, *283*, 631–638. [[CrossRef](#)]
111. Li, K.; Javed, H.; Zhang, G. *Calculation of Ozone and NO_x Production under AC Corona Discharge in Dry Air Used for Faults Diagnostic*; Atlantis Press: Amsterdam, The Netherlands, 2016. [[CrossRef](#)]
112. Amouroux, J.; Cavadias, S. Process and Installation for Heating a Fluidized Bed by Plasma Injection. 1984. Available online: www.osti.gov (accessed on 14 October 2023).
113. Rodygin, K.S.; Vikenteva, Y.A.; Ananikov, V.P. Calcium-Based Sustainable Chemical Technologies for Total Carbon Recycling. *ChemSusChem* **2019**, *12*, 1483–1516. [[CrossRef](#)] [[PubMed](#)]
114. Gicquel, A.; Cavadias, S.; Amouroux, J. Heterogeneous Catalysis in Low-Pressure Plasmas. *J. Phys. D Appl. Phys.* **1986**, *19*, 2013–2042. [[CrossRef](#)]
115. Sun, Q.; Zhu, A.; Yang, X.; Niu, J.; Xu, Y. Formation of NO_x from N₂ and O₂ in Catalyst-Pellet Filled Dielectric Barrier Discharges at Atmospheric Pressure. *Chem. Commun.* **2003**, *12*, 1418–1419. [[CrossRef](#)] [[PubMed](#)]
116. Pei, X.; Li, Y.; Luo, Y.; Man, C.; Zhang, Y.; Lu, X.; Graves, D.B. Nitrogen Fixation as NO_x Using Air Plasma Coupled with Heterogeneous Catalysis at Atmospheric Pressure. *Plasma Process. Polym.* **2023**, *21*, 2300135. [[CrossRef](#)]
117. O'Hare, L.R. Nitrogen Fixation by Plasma and Catalyst. 1984. Available online: www.osti.gov (accessed on 21 June 2023).
118. O'Hare, L.R. Nitrogen Fixation by Electric Arc and Catalyst. Available online: <https://patents.google.com/patent/US4877589A/en> (accessed on 21 June 2023).
119. Lei, X.; Cheng, H.; Nie, L.; Xian, Y.; Lu, X.P. Plasma-Catalytic NO_x Production in a Three-Level Coupled Rotating Electrodes Air Plasma Combined with Nano-Sized TiO₂. *J. Phys. D Appl. Phys.* **2021**, *55*, 115201. [[CrossRef](#)]
120. Belova, V.M.; Eremin, E.N.; Maltsev, A.N. Heterogeneous catalytic oxidation of nitrogen in a glow discharge II 1: 1 nitrogen-oxygen mixture. *Russ. J. Phys. Chem.* **1978**, *52*, 968–970.

121. Alamaro, M. Production of Nitric Oxides. Available online: <https://patents.google.com/patent/US4287040> (accessed on 21 June 2023).
122. Bayer, B.N.; Bruggeman, P.J.; Bhan, A. NO Formation by N₂/O₂ Plasma Catalysis: The Impact of Surface Reactions, Gas-Phase Reactions, and Mass Transport. *Chem. Eng. J.* **2024**, *482*, 149041. [[CrossRef](#)]
123. Yu, S.; Cornelis, S.; von Keudell, A. Controlled Synthesis of NO in an Atmospheric Pressure Plasma by Suppressing NO Destruction Channels by Plasma Catalysis. *J. Phys. D Appl. Phys.* **2024**, *57*, 245203. [[CrossRef](#)]
124. Kim, H.-H.; Teramoto, Y.; Ogata, A.; Takagi, H.; Nanba, T. Atmospheric-Pressure Nonthermal Plasma Synthesis of Ammonia over Ruthenium Catalysts. *Plasma Process. Polym.* **2016**, *14*, 1600157. [[CrossRef](#)]
125. Carman, R.J.; Kane, D.M.; Ward, B.K. Enhanced Performance of an EUV Light Source ($\lambda = 84$ nm) Using Short-Pulse Excitation of a Windowless Dielectric Barrier Discharge in Neon. *J. Phys. D Appl. Phys.* **2009**, *43*, 025205. [[CrossRef](#)]
126. Popov, N.A. Dissociation of Nitrogen in a Pulse-Periodic Dielectric Barrier Discharge at Atmospheric Pressure. *Plasma Phys. Rep.* **2013**, *39*, 420–424. [[CrossRef](#)]
127. A High Voltage Nanosecond Pulser with Variable Pulse Width and Pulse Repetition Frequency Control for Nonequilibrium Plasma Applications. IEEE Conference Publication. IEEE Xplore. Available online: <https://ieeexplore.ieee.org/document/7012774> (accessed on 14 October 2023).
128. Anastasopoulou, A.; Wang, Q.; Hessel, V.; Lang, J. Energy Considerations for Plasma-Assisted N-Fixation Reactions. *Processes* **2014**, *2*, 694–710. [[CrossRef](#)]
129. Jianli, Z.; Juncheng, Z.; Ji, S.; Hongchen, G.; Xiangsheng, W.; Weimin, G. Scale-up Synthesis of Hydrogen Peroxide from H₂/O₂ with Multiple Parallel DBD Tubes. *Plasma Sci. Technol.* **2009**, *11*, 181–186. [[CrossRef](#)]
130. Yao, S.; Fushimi, C.; Kodama, S.; Yamamoto, S.; Mine, C.; Fujioka, Y.; Madokoro, K.; Naito, K.; Kim, Y.-H. On the Scale-up of Uneven DBD Reactor on Removal of Diesel Particulate Matter. *Int. J. Chem. React. Eng.* **2009**, *7*. [[CrossRef](#)]
131. Anastasopoulou, A.; Butala, S.; Patil, B.; Suberu, J.; Fregene, M.; Lang, J.; Wang, Q.; Hessel, V. Techno-Economic Feasibility Study of Renewable Power Systems for a Small-Scale Plasma-Assisted Nitric Acid Plant in Africa. *Processes* **2016**, *4*, 54. [[CrossRef](#)]
132. Anastasopoulou, A.; Butala, S.; Lang, J.; Hessel, V.; Wang, Q. Life Cycle Assessment of the Nitrogen Fixation Process Assisted by Plasma Technology and Incorporating Renewable Energy. *Ind. Eng. Chem. Res.* **2016**, *55*, 8141–8153. [[CrossRef](#)]

Disclaimer/Publisher’s Note: The statements, opinions and data contained in all publications are solely those of the individual author(s) and contributor(s) and not of MDPI and/or the editor(s). MDPI and/or the editor(s) disclaim responsibility for any injury to people or property resulting from any ideas, methods, instructions or products referred to in the content.